Nano Research
DOI 10.1007/s12274-017-1713-1
Research Article
ISSN 1998-0124
CN 11-5974/O4

Oxidation layering mechanism of graphene-like MoS_2 prepared by the intercalation-detonation method

Fan Yang[1,2], Kuaishe Wang[1,2], Ping Hu[1,2,3] (✉), Zhenyu Chen[1,2], Jie Deng[1,2], Boliang Hu[1,2], Weicheng Cao[3], Dongxin Liu[3], Geng An[3], and Alex A. Volinsky[4]

[1] *School of Metallurgy Engineering, Xi'an University of Architecture and Technology, Xi'an 710055, China*
[2] *State Local Joint Engineering Research Center for Functional Materials Processing, Xi'an University of Architecture and Technology, Xi'an 710055, China*
[3] *Jinduicheng Molybdenum Co., Ltd., Xi'an 710077, China*
[4] *Department of Mechanical Engineering, University of South Florida, Tampa, FL 33620, USA*

Received: 6 April 2017
Revised: 9 June 2017
Accepted: 10 June 2017

KEYWORDS
graphene-like MoS_2, oxidation layering mechanism, intercalation-detonation, B_{1u} and A_{1g} peaks, Raman vibration mode

ABSTRACT

Graphene-like MoS_2 has attracted significant interest because of its unique electronic, optical, and catalytic properties with two-dimensional lamellar structure. Three kinds of intercalated MoS_2 samples were prepared using different oxidation layering methods, which are the first steps of intercalation-detonation. The oxidation layering mechanism of graphene-like MoS_2 was systematically characterized using Fourier transform infrared, X-ray photoelectron, and Raman spectroscopy techniques. The bulk MoS_2 sample was gradually oxidized from the edge to the interlayer in the presence of concentrated H_2SO_4 and $KMnO_4$. A large number of hydroxyl groups were bonded to the sulfur atom layer, forming S–OH bonds in the basal planes of the MoS_2 structure. The addition of deionized water to concentrated H_2SO_4 generated a large amount of heat, promoting the generation of more S–OH bonds, destroying residual Van der Waals forces between the layers, and finally stripping off parts of the flakes. The continuous addition of deionized water in the high temperature stage resulted in the largest oxidative intercalation effect. Additionally, the η factor was determined to compare the intensities of B_{1u} and A_{1g} peaks in the Raman spectra and quantify the effect of oxidative intercalation. The highest value of η was obtained when deionized water was added continuously during the preparation of intercalated MoS_2.

1 Introduction

Layered materials have recently attracted considerable attention because of their exotic electronic properties and high specific surface area, which are important for sensing, catalysis, and energy storage applications.

Address correspondence to huping1985@126.com

Graphene is one of the most well known layered materials; transition metal dichalcogenides (TMDs), transition metal oxides, and other two-dimensional (2D) compounds are also widely used [1]. Molybdenum disulfide (MoS_2) is one of the most studied TMDs because of its superior optical and electronic properties [2]. In the bulk form, MoS_2 has a layered structure with strong covalent bonding in each layer and weak Van der Waals bonding between the layers. Each layer has a thickness of 6.5 Å. The S–Mo–S bonds form a sandwich structure of MoS_2 wherein two hexagonal planes of S atoms are separated by a plane of Mo atoms [3, 4]. Unlike graphene which is an excellent conductor, bulk crystalline MoS_2 is a semiconductor with an indirect band gap of approximately 1.2 eV, which gradually increases with decrease in the number of layers. Atomically layered graphene-like MoS_2 is a semiconductor material with a direct band gap, and the band gap of single-layer MoS_2 is 1.9 eV [5–7].

Owing to the adjustable band gap, graphene-like MoS_2 has significant potential for applications in photoelectronic devices. However, it is difficult to obtain high-purity graphene-like MoS_2 structures using conventional methods, such as micromechanical exfoliation, Li^+ intercalation, liquid ultrasonic, and chemical vapor deposition [8–12]. Furthermore, other factors, such as small-scale preparation, poor repeatability, time consumption, low efficiency, and product quality hinder the development of this attractive material. Thus, reproducible production of graphene-like nanosheets in bulk quantities is still a challenge. With the rapid development of various ultrathin MoS_2-based devices, unique properties characterization and easy identification methods have emerged. Raman spectroscopy, X-ray photoelectron spectroscopy (XPS), high-resolution transmission electron microscopy, scanning tunneling microscopy, and other advanced techniques have been used to characterize this promising layered material. For decades, Raman spectroscopy has been used to study the different crystalline structures of MoS_2, and various phonons vibration modes have been identified. For example, Chen et al. [13] observed the longitudinal acoustic phonons at the M point (LA(M)) at approximately 460 cm^{-1} in 1974. The in-plane E^1_{2g} and the out-of-plane A_{1g} vibration modes were observed by Bertrand et al. [14] in 1992. Recently, Lee et al. [15] and Li et al. [16] reported two opposite points of view regarding the E^1_{2g} and the A_{1g} vibration modes. According to Lee et al., the frequencies, intensities, and widths of the E^1_{2g} and the A_{1g} peaks depend on the layer thickness of ultrathin MoS_2 flakes. Whereas, Li et al. proposed that the Raman frequencies of the E^1_{2g} and A_{1g} peaks vary monotonously with the number of layers in ultrathin MoS_2 flakes and can be used as reliable features to identify the number of layers. Furthermore, other lesser-known second order modes, such as Raman-inactive E^2_{1u} and B_{1u}, have been observed by resonance Raman spectroscopy [17].

A novel intercalation-detonation method to prepare graphene-like MoS_2 was reported in our previous study [18], wherein for the first time, oxygen-containing groups were used as intercalation compounds of layered structures and explosion technology was used to exfoliate the intercalated MoS_2.

In this paper, we systematically studied the oxidation layering mechanism of graphene-like MoS_2 by Fourier transform infrared spectroscopy, XPS, and Raman spectroscopy. In order to validate the proposed mechanism, three kinds of intercalated MoS_2 samples were prepared using different oxidation layering methods by varying the method of addition of water. Most importantly, we determined the factor η, which is the ratio of the intensities of B_{1u} and A_{1g} peaks in the Raman spectrum, to quantify the extent of oxidative intercalation.

2 Experimental

2.1 Intercalation process

Pure analytical grade MoS_2 powder, $NaNO_3$, and $KMnO_4$ were used as the raw materials, and 98% concentrated sulfuric acid was used to oxidize bulk MoS_2. Three kinds of preparation methods were used to study the intercalation mechanism of MoS_2.

The typical procedure used for the preparation of intercalated MoS_2 is described as follows. The MoS_2 powder and the $NaNO_3$ crystals were dissolved in a certain volume of 98% concentrated sulfuric acid in the mass ratio of 2:1; the concentration of MoS_2 powder dispersed in concentrated sulfuric acid was 0.25 g/mL. The reaction flask was placed in an ice

bath with violent stirring, and a certain quantity of $KMnO_4$ (three times the mass of MoS_2 powder) was added slowly to avoid a sudden increase in the temperature. After a reaction time of 120 min, the flask was heated to 35 ℃ for 60 min and then maintained at 90 ℃ for 5 min. The reactive solution was diluted during stirring, and a certain amount of warm deionized water was added slowly during the heating-up process from 35 to 90 ℃. A 5% hydrogen peroxide solution was added to the solution after the heating process to remove the $KMnO_4$. Subsequently, the solution was vacuum filtered and thoroughly washed with deionized water until the pH of the filtrate became neutral. Intercalated MoS_2 was obtained after the filtration.

Three different methods of addition of deionized water were used to prepare the intercalated MoS_2 flakes. In method 1, deionized water of the same volume as sulfuric acid was added to the solution during the reaction at 35 ℃. In method 2, deionized water was continuously added to the solution during the heating-up process from 35 to 90 ℃. In method 3, deionized water was added to the solution during the heating-up process from 35 to 90 ℃ and during the holding step at 90 ℃.

2.2 Spectroscopic analyses

Raman spectroscopy (Jobin Yvon HR-800) was performed using a HeNe laser with an excitation wavelength of 632.8 nm. The XPS (PHI-5400) measurements were performed using monochromatic aluminum KR X-rays. The Thermo Scientific™ Advantage software was used for the XPS data analyses. The FT-IR measurements (Nicolet iN10 MX) were performed using the KBr tablet method in the scan range of 400–4,000 cm^{-1}.

3 Results and discussion

3.1 FT-IR spectra of the intercalated MoS_2 samples

Figure 1 shows the FT-IR spectra of the intercalated MoS_2 samples prepared using the three different methods along with that of bulk MoS_2. High-intensity peaks at approximately 1,640 and 3,400 cm^{-1} were observed in both the bulk and the intercalated MoS_2 samples, and the intensity of the peaks increased from the bulk to the intercalated MoS_2. The peaks at 1,640 cm^{-1} and 3,000–3,800 cm^{-1} correspond to water bending and hydroxyl stretching vibration modes, respectively. These results indicate that a small amount of water exists in the bulk MoS_2 sample, while a higher amount of water and hydroxyl groups exist in the intercalated MoS_2 samples. In addition, a peak at approximately 1,100 cm^{-1} was observed in all the intercalated MoS_2 samples except the bulk MoS_2 sample, and the intensity of this peak increased from methods 1 to 3. The peak at 1,030–1,400 cm^{-1} denotes the S=O stretching vibration. Therefore, the effect of oxidative intercalation increases from methods 1 to 3.

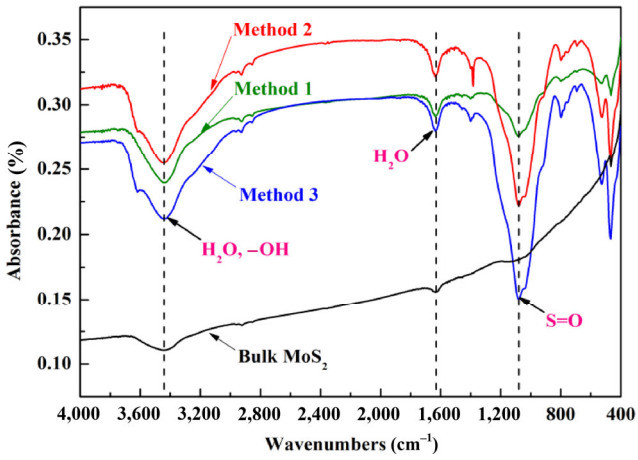

Figure 1 FT-IR spectra of the bulk and the intercalated MoS_2 samples.

3.2 XPS spectra of the intercalated MoS_2 samples

The XPS measurements were carried out to characterize the chemical compositions of the bulk and the intercalated MoS_2 samples, and the results are shown in Fig. 2. The high-resolution Mo 3d and S 2p spectra showed peaks corresponding to the Mo 3d3/2, Mo 3d5/2, S 2p1/2, and S 2p3/2 components of MoS_2, respectively (Figs. 2(a) and 2(b)) [19].

The high-resolution O 1s spectrum of the bulk MoS_2 sample, as shown in Fig. 2(c) shows a peak at 532.1 eV, which is associated with the hydroxyl group formed by dissociation of water. The O 1s spectrum of the intercalated MoS_2 samples shows a peak at 533 eV, which is related to the S–OH bond [20]. This indicates that the oxygen-containing functional groups were bonded to the surface or the sulfur atom layer of MoS_2

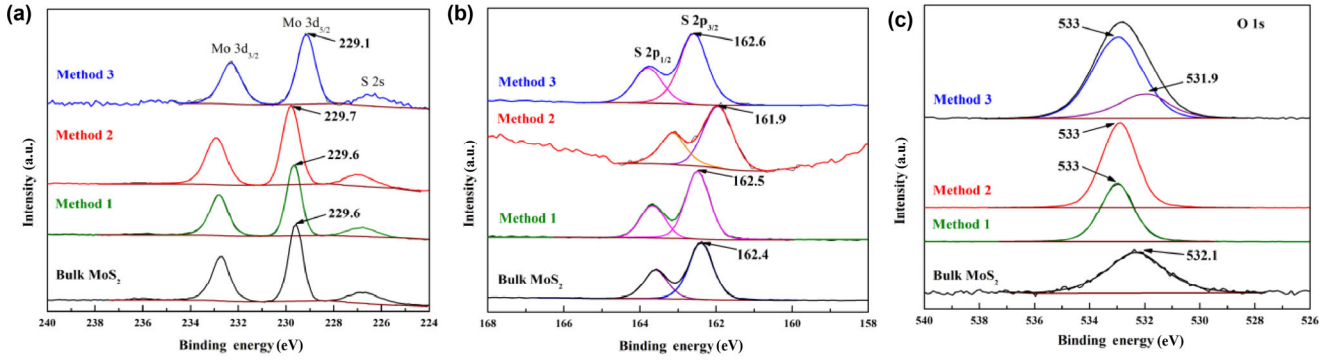

Figure 2 XPS spectra of the bulk and the intercalated MoS_2 samples. (a) High-resolution Mo 3d spectra, (b) high-resolution S 2p spectra, and (c) high-resolution O 1s spectra.

during the three different intercalation processes. The weak peak observed at 531.9 eV in the intercalated MoS_2 sample prepared using method 3, is related to rudimental dissociation of water. Additionally, the intensity of the peak at 533 eV increased from methods 1 to 3, which indicates that the amount of S–OH bonds and the effect of oxidative intercalation increased from methods 1 to 3.

3.3 Raman spectra of intercalated MoS_2 samples

Raman spectroscopy was used to characterize the vibration frequencies of the atoms of the bulk and the intercalated MoS_2 samples, and the results are shown in Fig. 3. The MoS_2 samples showed peaks at approximately 383 and 405 cm^{-1} corresponding to the vibration modes of E^1_{2g} and A_{1g}, respectively, consistent with previously reported results [1]. Besides, a peak

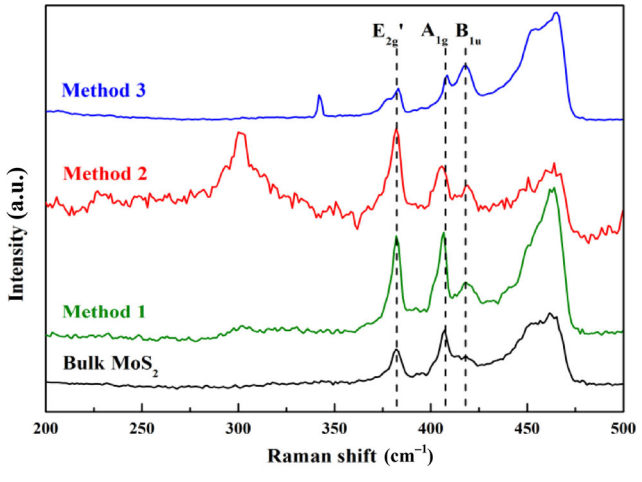

Figure 3 Raman spectra of the bulk and the intercalated MoS_2 samples.

near the A_{1g} mode at approximately 415 cm^{-1} was observed in the Raman spectra of the bulk and the intercalated MoS_2 samples. This peak corresponds to the vibrational B_{1u} mode and is consistent with that reported in the literature [16]. The intensity ratio of B_{1u} and A_{1g} peaks was calculated to be 0.61, 0.68, 0.87, and 1.15 for the bulk MoS_2 and the intercalated MoS_2 samples prepared using methods 1 to 3, respectively. Combining the results of FT-IR spectroscopy and XPS, it can be confirmed that the effect of oxidative intercalation increases from methods 1 to 3. In addition, the intensity ratio of B_{1u} and A_{1g} peaks in the Raman spectra increased from methods 1 to 3. This is attributed to the effect of oxidative intercalation, in which oxygen-containing groups are inserted into the MoS_2 layer, and the spacing between the layers is increased. This change in the layer structure induces the evolution of the vibrational mode at 415 cm^{-1}, and the intensity ratio of B_{1u} and A_{1g} peaks corresponds to the degree of oxidative intercalation.

The B_{1u} vibration mode originates from the shoulder of the A_{1g} peak in bulk MoS_2, which evolves into a separate peak at 415 cm^{-1} with the variety of MoS_2 layers. Previous literature [17] reports that the peak at 415 cm^{-1} originates from the B_{1u} Raman-inactive mode because of a two-phonon scattering process involving longitudinal quasi-acoustic phonons and transverse optical phonons. We define the intensity ratio of B_{1u} and A_{1g} peaks as a factor η, which represents the layer spacing and the amount of bonds in the MoS_2 flakes that causes a change in the intensity of the two-phonon scattering process. The intensity ratio η is expressed as

$$\eta = \frac{I_{B1u}}{I_{A1g}} \quad (1)$$

where I_{B1u} is the intensity of the B_{1u} peak and I_{A1g} is the intensity of the A_{1g} peak. Thus, the intercalated sample obtained using method 3 exhibits the highest value of η, and consequently, the best oxidative intercalation effect.

3.4 Mechanism of oxidative intercalation

The results of the present study show that the effect of oxidative intercalation increased from methods 1 to 3. The difference between methods 1 to 3 is the method of addition of deionized water. The deionized water was added to the solution during the reaction at 35 ℃ in method 1, it was continuously added to the solution during the heating-up process from 35 to 90 ℃ in method 2, and it was added to the solution during the heating-up process from 35 to 90 ℃ and during the holding step at 90 ℃ in method 3.

The proposed mechanism of oxidative intercalation of bulk MoS_2 is shown in Fig. 4. In the low-temperature stage, the strong oxidants concentrated H_2SO_4 and $KMnO_4$ were adsorbed on the MoS_2 edges, and the edges were oxidized and intercalated by the generated hydroxyl and other oxygen-containing groups. The oxygen-containing groups reduced the intermolecular force between the layers at the edges and increased the layer spacing of the MoS_2 flakes.

In the mid-temperature stage, with the rise in the reaction temperature, the oxidation effect of concentrated H_2SO_4 and $KMnO_4$ gradually increased, resulting in the generation of more oxygen-containing groups between the MoS_2 layers. With further increase in the lamellar spacing, the oxidant gradually penetrated to the inner layer.

In the high-temperature stage, the oxidation effect of concentrated H_2SO_4 further increased because of the high reaction temperature, causing more hydroxyl groups bonded to the sulfur atom layer to form S–OH bonds in the basal planes of the MoS_2 structure. On the other hand, the dilution of concentrated H_2SO_4 with deionized water in methods 2 and 3 was exothermic, which promoted the generation of S–OH bonds, destroyed the residual Van der Waals forces between the layers, and finally stripped off parts of the flakes. Furthermore, the addition of deionized water also reduced the temperature of the concentrated H_2SO_4 core during the holding step at 90 ℃ in method 3, preventing oxidative damage of the MoS_2 layered structure.

Finally, the bulk MoS_2 was oxidized and intercalated. Parts of the oxidation-intercalated MoS_2 flakes were stripped off, forming graphene-like MoS_2. Other large-sized MoS_2 flakes are waiting to be exfoliated by subsequent exfoliation process.

4 Conclusion

In summary, we systematically investigated the

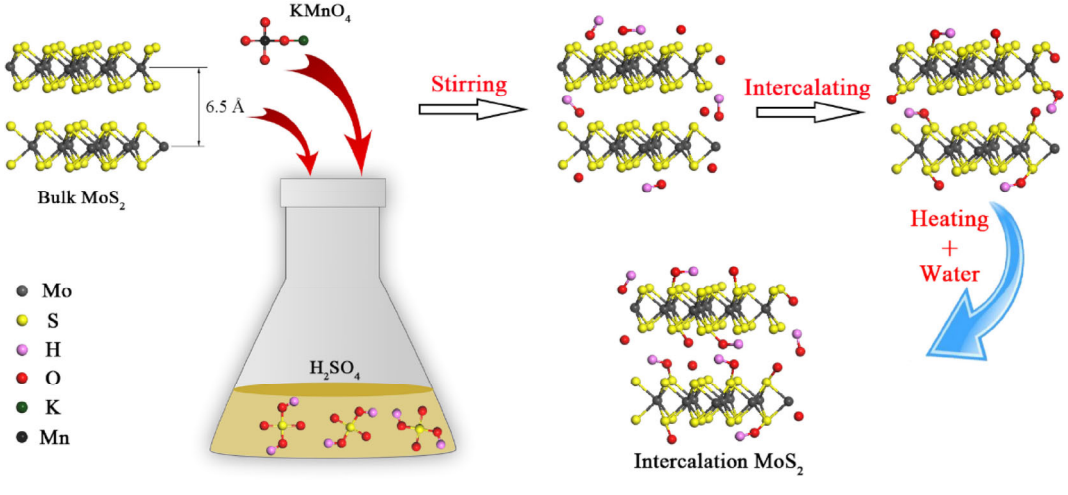

Figure 4 Schematic illustration of the oxidation layering mechanism.

oxidation layering mechanism of graphene-like MoS_2 by using FT-IR, XPS, and Raman spectroscopy techniques. In order to validate the proposed mechanism, three kinds of intercalated MoS_2 samples were prepared using different oxidation layering methods by varying the method of addition of water. The FT-IR spectroscopy and the XPS results showed that the method of addition of deionized water significantly affected the degree of oxidative intercalation of the MoS_2 samples. The bulk MoS_2 sample was gradually oxidized from the edge to the interlayer by the addition of concentrated H_2SO_4 and $KMnO_4$, and a large amount of hydroxyl groups were bonded to the sulfur atom layer, forming S–OH bonds in the basal planes of the MoS_2 structure. The addition of deionized water to concentrated H_2SO_4, which was exothermic, promoted the formation of more S–OH bonds, destroyed the residual Van der Waals forces between the layers, and finally stripped off parts of the flakes. Most importantly, the intensity ratio of B_{1u} and A_{1g} peaks in the Raman spectra, η, was determined to quantify the effect of oxidative intercalation. The highest value of η was obtained for the method in which deionized water was added continuously during the preparation of intercalated MoS_2.

Acknowledgements

This research was supported by the National Natural Science Foundation of China (NSFC, No. 51404181), Outstanding Doctorate Dissertation Cultivation Fund of Xi'an University of Architecture and Technology (No. 6040317013), Youth Science and Technology New Star Project of Shaanxi Province Innovation Ability Support Plan (No. 2017KJXX-63), China Postdoctoral Science Foundation (No. 2016M600770), and Postdoctoral Work Centre in Jinduicheng Molybdenum Co., Ltd. (No. 2016-19).

References

[1] Coleman, J. N.; Lotya, M.; O'Neill, A.; Bergin, S. D.; King, P. J.; Khan, U.; Young, K.; Gaucher, A.; De, S.; Smith, R. J. et al. Two-dimensional nanosheets produced by liquid exfoliation of layered materials. *Science* **2011**, *331*, 568–571.

[2] Macmahon, D.; Brothers, A.; Florent, K.; Kurinec, S. Layered structure of MoS_2 investigated using electron energy loss spectroscopy. *Mater. Lett.* **2015**, *161*, 96–99.

[3] Radisavljevic, B.; Radenovic, A.; Brivio, J.; Giacometti, V.; Kis, A. Single-layer MoS_2 transistors. *Nat. Nanotechnol.* **2011**, *6*, 147–150.

[4] Li, X.; Li, J. H.; Wang, X. H.; Hu, J. X.; Fang, X.; Chu, X. Y.; Wei, Z. P.; Shan, J. J.; Ding, X. C. Preparation, applications of two-dimensional graphene-like molybdenum disulfide. *Integr. Ferroelectr.* **2014**, *158*, 26–42.

[5] Huang, Y.; Wu, J.; Xu, X. F.; Ho, Y.; Ni, G. X.; Zou, Q.; Koon, G. K. W.; Zhao, W. J.; Neto, A. H. C.; Eda, G. et al. An innovative way of etching MoS_2: Characterization and mechanistic investigation. *Nano Res.* **2013**, *6*, 200–207.

[6] Zhan, Y. J.; Liu, Z.; Najmaei, S.; Ajayan, P. M.; Lou, J. Large-area vapor-phase growth and characterization of MoS_2 atomic layers on a SiO_2 substrate. *Small* **2012**, *8*, 966–971.

[7] Dolui, K.; Rungger, I.; Das Pemmaraju, C.; Sanvito, S. Possible doping strategies for MoS_2 monolayers: An *ab initio* study. *Phys. Rev. B* **2013**, *88*, 075420.

[8] Yoon, Y.; Ganapathi, K.;Salahuddin, S. How good can monolayer MoS_2 transistors Be? *Nano Lett.* **2011**, *11*, 3768–3773.

[9] Joensen, P.; Frindt, R. F.; Morrison, S. R. Single-layer MoS_2. *Mater. Res. Bull.* **1986**, *21*, 457–461.

[10] Liu, K. K.; Zhang, W. J.; Lee, Y. H.; Lin, Y. C.; Chang, M. T.; Su, C. Y.; Chang, C. S.; Li, H.; Shi, Y. M.; Zhang, H. et al. Growth of large-area and highly crystalline MoS_2 thin layers on insulating substrates. *Nano Lett.* **2012**, *12*, 1538–1544.

[11] Luo, H.; Xu, C.; Zou, D. B.; Wang, L.; Ying, T. K. Hydrothermal synthesis of hollow MoS_2 microspheres in ionic liquids/water binary emulsions. *Mater. Lett.* **2008**, *62*, 3558–3560.

[12] Pol, V. G.; Pol, S. V.; George, P. P.; Gedanken, A. Combining MoS_2 or $MoSe_2$ nanoflakes with carbon by reacting $Mo(CO)_6$ with S or Se under their autogenic pressure at elevated temperature. *J. Mater. Sci.* **2008**, *43*, 1966–1973.

[13] Chen, J. M.; Wang, C. S. Second order Raman spectrum of MoS_2. *Solid State Commun.* **1974**, *14*, 857–860.

[14] Bertrand, P. A. Surface-phonon dispersion of MoS_2. *Phys. Rev. B* **1991**, *44*, 5745–5749.

[15] Lee, C.; Yan, H. G.; Brus, L. E.; Heinz, T. F.; Hone, J.; Ryu, S. Anomalous lattice vibrations of single- and few-layer MoS_2. *ACS Nano* **2010**, *4*, 2695–2700.

[16] Li, H.; Zhang, Q.; Yap, C. C. R.;Tay, B. K.; Edwin, T. H. T.; Olivier, A.; Baillargeat, D. From bulk to monolayer MoS_2: Evolution of Raman scattering. *Adv. Funct. Mater.* **2012**, *22*, 1385–1390.

[17] Sekine, T.; Uchinokura, K.; Nakashizu, T.; Matsuura, E.; Yoshizaki, R. Dispersive Raman mode of layered compound 2H-MoS_2 under the resonant condition. *J*. *Phys*. *Soc*. *Jpn*. **1984**, *53*, 811–818.

[18] Yang, F.; Hu, P.; Wang, K. S.; Chen, Z. Y.; Hu, B. L.; Song, R.; Li, Q. W.; Cao, W. C.; Liu, D. X.; An, G. et al. Graphene-like MoS_2 prepared by a novel intercalation-detonation method. *Mater*. *Lett*. **2017**, *188*, 224–227.

[19] Wang, P. P.; Sun, H. Y.; Ji, Y. J.; Li, W. H.; Wang, X. Three-dimensional assembly of single-layered MoS_2. *Adv*. *Mater*. **2014**, *26*, 964–969.

[20] Zhang, Y.; Chen, P.; Wen, F. F.; Yuan, B.; Wang, H. G. Fe_3O_4 nanospheres on MoS_2nanoflake: Electrocatalysis and detection of Cr(VI) and nitrite. *J*. *Electroanal*. *Chem*. **2016**, *761*, 14–20.